Analysis on the Potential Performance of GPS and Galileo Precise Point Positioning using simulated Real-Time products.

Francesco Basile, Terry Moore, Chris Hill

Nottingham Geospatial Institute, University of Nottingham

Email: Francesco.Basile@nottingham.ac.uk

Abstract

With the evolving Global Navigation Satellite System (GNSS) landscape, the International GNSS Service (IGS) has started the Multi-GNSS Experiment (MGEX) to produce precise products for new generation systems. Various Analysis Centres are working on the estimation of precise orbits, clocks and bias for Galileo, Beidou and QZSS satellites. However, at the moment this products can only be used for post-processing applications. Indeed the IGS Real-Time service only broadcasts GPS and GLONASS corrections. In this research, a simulator of Multi-GNSS observations and Real-Time precise products has been developed to analyse the performance of GPS only, Galileo only and GPS plus Galileo Precise Point Positioning. The error models in the simulated orbits and clocks were based on the difference between the GPS Real-Time and the Final products. Multiple scenarios were analysed, considering different signal combined in the Ionosphere Free linear combination. Results in a simulated open area environment show better performance of the Galileo only case over the GPS only case. Indeed, up 33% and 29% of improvement, respectively, in the accuracy level and convergence time can be observed when using the full Galileo constellation compared to GPS. The dual constellation case provides good improvements, in particular in the convergence time (47% faster than GPS). This paper will also consider the impact of different linear combinations of the Galileo signals, and the potential of the E5 AltBOC signal. Even though it is significantly more precise than E5a, the PPP performance obtained with the Galileo E1-E5a combination is either better or similar to the one with Galileo E1-E5. The reason of this inconsistency was found in the use of the ionosphere free combination with E1. Finally alternative methods of ionosphere error mitigation are considered in order to ensure the best possible positioning performance from the Galileo E5 signal in multi-frequency PPP.

1 Introduction

Precise Point Positioning (PPP) (Zumberge et al., 1997) is a positioning techniques that can achieve decimetre to centimetre level accuracy by using undifferenced pseudorange and carrier phase measurements from a single Global Navigation Satellite System (GNSS) satellite. In contrast to differential GNSS techniques, PPP extends the concept of high accuracy GNSS to remote areas where no reference stations are available. However, the long convergence or reconvergence time (15 to 60 minutes) strongly limits its applicability.

In PPP the satellites' orbits and clocks information broadcast in the navigation message are replaced by precise products estimated in a network solution. Beside commercial services, the International GNSS Service (IGS) has provided, free of charge, products for GPS since 1994 and for GLONASS since 2000. With the evolving GNSS landscape, IGS has started a Multi – GNSS experiment (MGEX) to explore and promote the use of the new navigation signals and constellations (Montenbruck et al., 2014, Montenbruck et al., 2013, Rizos et al., 2013). The analysis centres (ACs) contributing to MGEX are currently providing Final and Rapid orbits and clocks for Galileo, Beidou and QZSS, as well as GPS and GLONASS. However, this products are only usable for post – processing applications. Indeed, the IGS Real – Time service only provides corrections to GPS and GLONASS. Those people who are interested into the potential PPP performance of the new systems in real – time can only rely on commercial providers.

The number of visible satellites is also a limiting factor to study the potentials of Galileo and Galileo plus GPS positioning. Today (November 2017), only 18 Galileo satellites are orbiting around the Earth and 15 of them are usable for positioning. Within the orbiting satellites, the Galileo GSAT 104 (PRN E20) was set to unavailable in May 2014 (GSA, 2014) following a power outage, while the GSAT 201 and GSAT 202 (PRN E18 and E14) are currently under testing (GSA, 2016a, GSA, 2016b) after they were recovered from the wrong orbit the two satellites were placed into (ESA, 2015). The full constellation is forecast to be ready by 2020.

Despite these limitations, significant research efforts have been made to analyse the potential benefits of Multi – GNSS in PPP both using simulated data (Juan et al., 2012, Shen and Gao,

2006) and real data (Miguez et al., 2016, Afifi and El-Rabbany, 2015). These developments demonstrated that, once Galileo will reach its final capability, the PPP convergence time will be reduced to more than a half when processing GPS and Galileo observations, from static receivers in open sky conditions.

2 Development of a Multi Constellation Multi frequency GNSS simulator

In order to evaluate what are the future performance of Galileo in PPP, on its own and together with GPS, in this research a Multi-Constellation GNSS simulator was developed in Simulink environment.

The inputs that are required to run a simulation are:

- Reference trajectory for user motion. It includes a time series of user's latitude, longitude and height at each epoch. In case the output data rate is higher than the input data rate, an interpolation between points is performed to obtain the user's position at the required epoch.
- Information about satellites motion and clocks' offset and drift. For GPS satellites, this information is obtained from the Yuma almanac; while for Galileo, the nominal orbital parameters of the Galileo constellation are used.
- Klobuchar parameters to model the Ionospheric delay.

The simulator outputs GNSS observations in Receiver Independent Exchange (RINEX) 2.11 observation format.

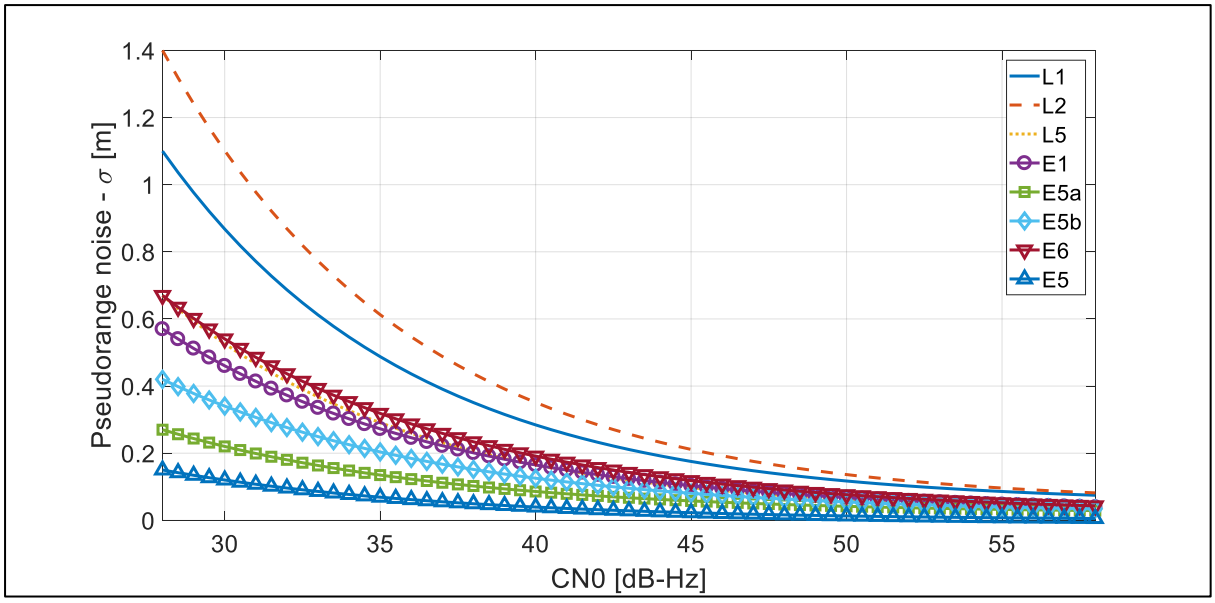

Figure 1. Receiver noise for different GPS and Galileo signals as function of the SNR (Richardson et al., 2016).

Code pseudoranges $P_{r,k}^s$ and carrier phases $L_{r,k}^s$ on frequency k, broadcast by satellite s and received by the receiver r, are simulated considering the main delays as shown in Teunissen and Montenbruck (2017).

$$P_{r,k}^s = g_r^s + c(\mathrm{d}t_r - dt^s + \delta t^{rel}) + c\left(d_{r,k} - d_k^s\right) + I_{r,k}^s + T_r^s + \varepsilon_{P,r,k}^s \quad (1)$$

$$L_{r,k}^s = g_r^s + c(\mathrm{d}t_r - dt^s + \delta t^{rel}) - I_{r,k}^s + T_r^s + \lambda_k N_{r,k}^s + \varepsilon_{L,r,k}^s \quad (2)$$

In equation 1 and 2, which are the generic measurement equations for pseudorange and carrier phase, figure: the geometric range g_r^s, the receiver and satellite clock offset $\mathrm{d}t_r$ and dt^s, the relativistic effect δt^{rel}, the speed of light c, the frequency dependant instrumental delays for receiver $(d_{r,k})$ and satellites (d_k^s), the atmospheric delays due to ionosphere $I_{r,k}^s$ and troposphere T_r^s, the carrier phase initial ambiguity $N_{r,k}^s$, the wavelength λ_k of the carrier signal on frequency k, and other errors like receiver noise and multipath ($\varepsilon_{P,r,k}^s$ and $\varepsilon_{L,r,k}^s$).

The pseudorange receiver noise ε_{PR} has been modelled as a white Gaussian noise (normally distributed with zero mean) with a standard deviation σ_{PR} depending on the signal to noise ratio (SNR). The model is based on the results presented in Richardson et al. (2016).

$$\varepsilon_{PR} = N(0, \sigma_{PR}^2) \quad (3)$$

The exponential law of σ_{PR} as function of the SNR is showed in Figure 1: Galileo pseudoranges seem to be less noisy than the GPS ones. The carrier phase are assumed to have a precision of 1 cm.

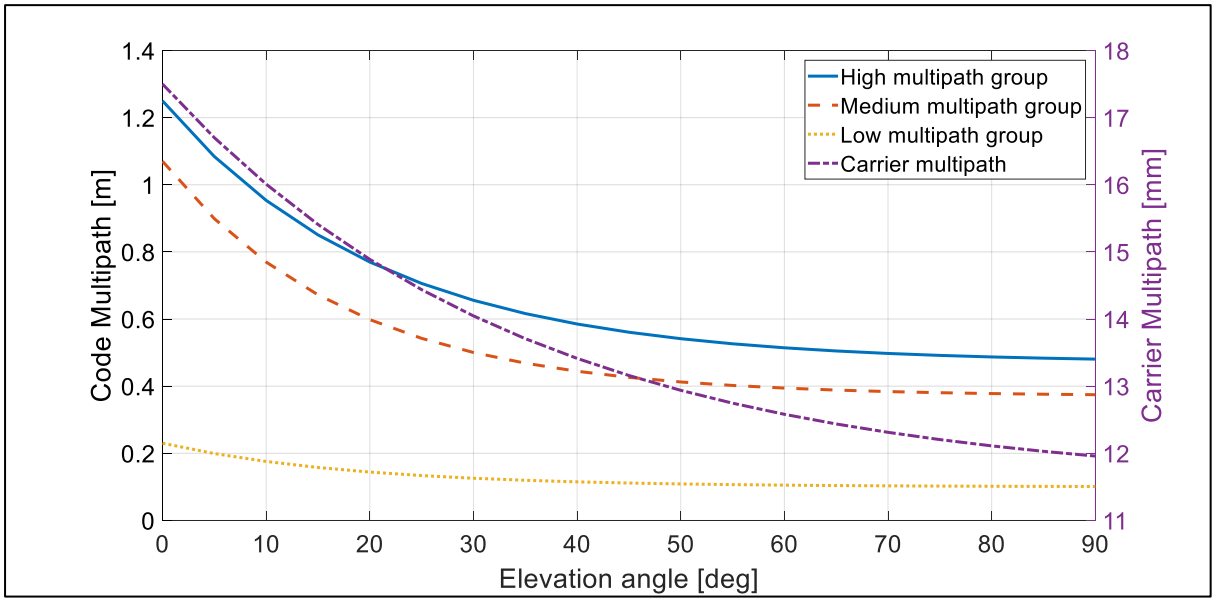

Figure 2. Magnitude of the multipath delays as function of the elevation angle. The high multipath group (blue) includes the Galileo E1 and E6 and GPS L1 and L2 pseudoranges. The medium multipath group (orange) includes the Galileo E5a, E5b and GPS L5 pseudoranges. The low multipath group (yellow) includes Galileo E5 pseudoranges. The multipath on the carrier phase measurements is also showed in purple.

Multipath is modelled as first order Gauss Markov process (O'Keefe et al., 2006) with a correlation time τ which depends on the type of simulation. It is larger for static scenarios, shorter for kinematic scenarios.

$$\varepsilon_{mp_k} = w_k + \varepsilon_{mp_{k-1}} e^{-\frac{\Delta t}{\tau}} \tag{4}$$

In Equation 4, ε_{mp_k} is the Gauss Markov process being generated at epoch k, Δt is the observation rate, and w_k is the driving noise term simulated using a normally distributed random number generator with a standard deviation that is assumed to be a function of the elevation angle of the satellite.

As illustrated in Simsky et al. (2008), the Galileo E1 and E6 and GPS L1 are the most affected by multipath, while Galileo E5 is the least affected. Based on these results, three multipath groups were defined: a high multipath group, which includes all the signals that are more sensitive to the multipath (Galileo E1, E6 and GPS L1, L2); a medium multipath group (Galileo E5a, E5b and GPS L5) and a low multipath group (Galileo E5). The standard deviation of the

assumed multipath for each group is showed in Figure 2 together with the assumed carrier phase multipath.

The simulator also outputs Real-Time quality precise orbits and clocks in Standard Products 3 (SP3) and RINEX clock 2.0 formats. The model to simulate the products' error is based on the comparison between the GPS IGS Real-Time and ESA Final products. Data relative to 4 weeks (GPS week 1917 to 1920) have been analysed in order to define a suitable model.

Table 1. RMS of the products' difference during the period analysed.

	Radial	**Along-track**	**Cross-track**	**Clocks**
RMS [cm]	1.60	3.41	1.91	19.40

The Crustal Dynamics Data Information System (CDDIS) archives products generated from real-time data stream in support of the IGS Real-Time Service. The precise orbits files are published in SP3 format at 30 seconds interval, while the precise clocks files are in RINEX clock format at 30 seconds interval. They are derived from IGC01 solution, which uses the real-time data streams that are referred to the satellite center-of-mass (CoM). The ESA Final orbits, which are published at 15 minutes interval, have been interpolated to reduce the data interval to 30 seconds.

Table 1 shows the RMS of the products' difference. The RMS of the clocks' difference are almost twice as large as those presented in Hadas and Bosy (2015), while the radial, cross-track and along-track orbital components have nearly the same RMS.

Figure 3 shows the daily time series of the orbital component differences for GPS 1 on the 2nd October 2016. These plots clearly show a periodic pattern on all components. Two peculiar patterns are also visible in the cross-track and along-track components. The authors could not explain what the reason is for this behaviour.

Figure 4 shows the difference between the IGS Real-Time clocks and the ESA Final clocks for GPS 1 on the 2nd October 2016. A drift is visible in the daily time series. This behaviour is related to the way the products are computed.

When estimating the clocks, a reference needs to be defined. The Final products are computed processing 7 days of data, the clock of a station at a particular epoch is considered as reference

for the computation of all the other clocks for that week. On the other hand, the Real-Time products are computed, independently, epoch by epoch. Therefore, while the reference clock for the Real-Time products is assumed to be zero at each epoch, in the Final products it drifts with the time. This drift is visible when differentiating the two type of precise clocks. To overcome this problem, single difference between satellites' clock is performed, in such a way that we always use the same satellite's clock as reference.

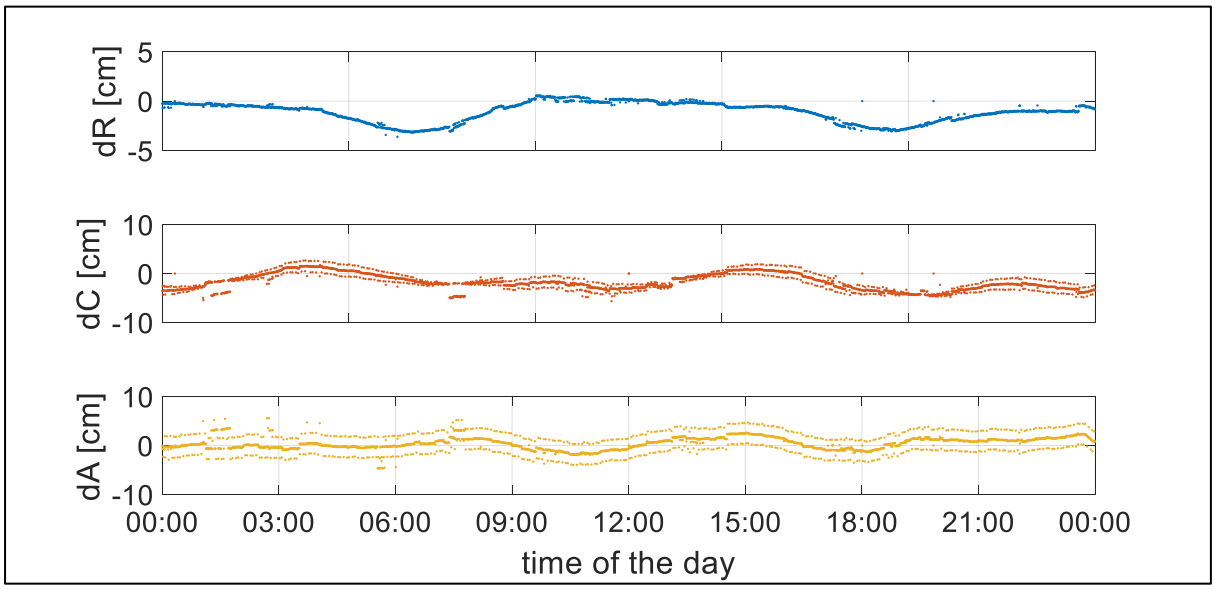

Figure 3. Difference between the IGS Real-Time and ESA Final orbits for GPS PRN 1 on the 2nd October 2016. The blue plot shows the products' difference in the radial component of the satellite's position, the orange plot show the difference in the cross-track component, while the yellow one shows the difference on the along-track component.

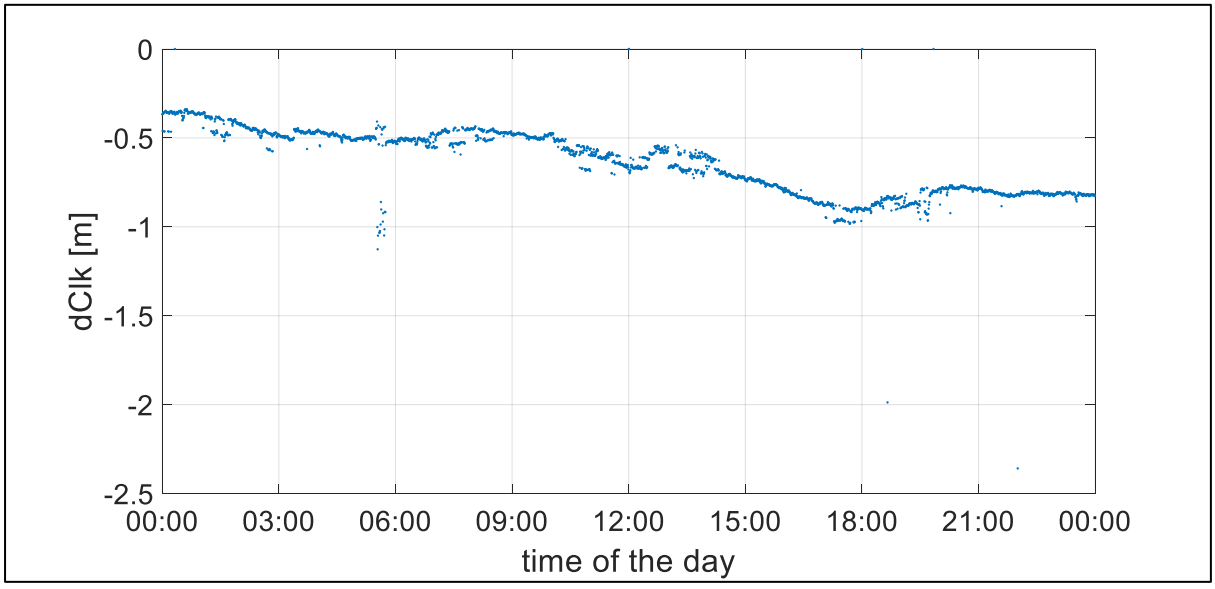

Figure 4. Difference between IGS Real-Time and ESA Final clocks for GPS PRN 1 on the 2nd October 2016.

Given the periodical nature of the products' errors, a fitting method based on the Fourier series was used to characterize them.

$$\Delta_{RT} = a_0 + \sum_n a_n \sin(n\omega t + \Phi_n) \tag{5}$$

In Equation 5, a_0 is the bias, a_n is the amplitude, $n\omega$ is the frequency and Φ_n is the phase of the sinusoid of order n.

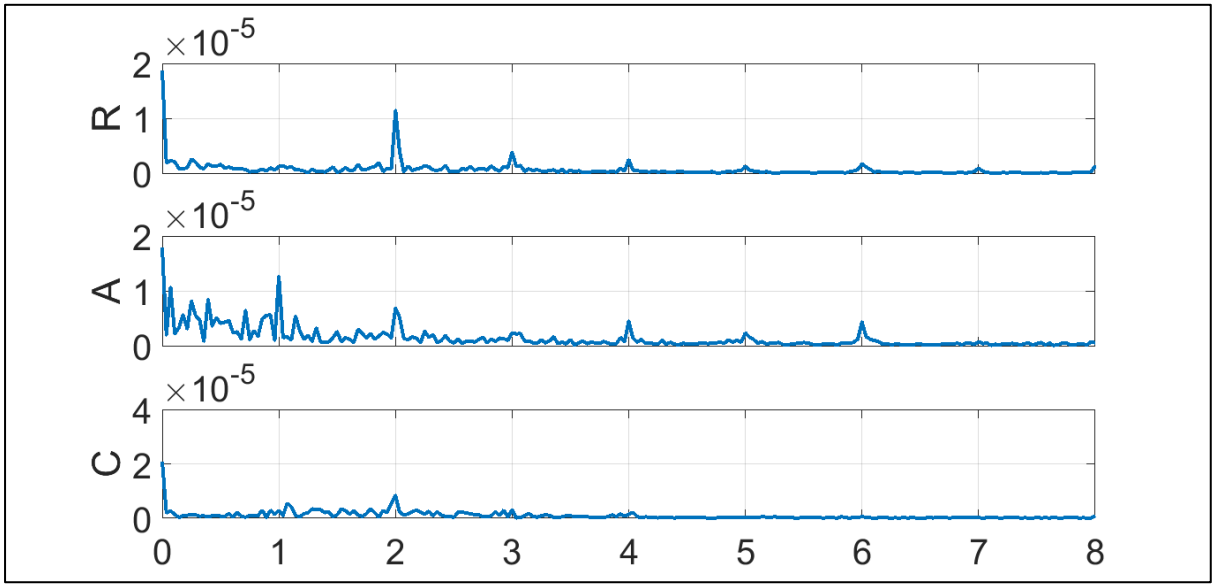

Figure 5. Spectrum of the error in the orbit components radial, along-track, and cross-track. PRN 5. On the x axis the frequencies are in unites of 1/ day.

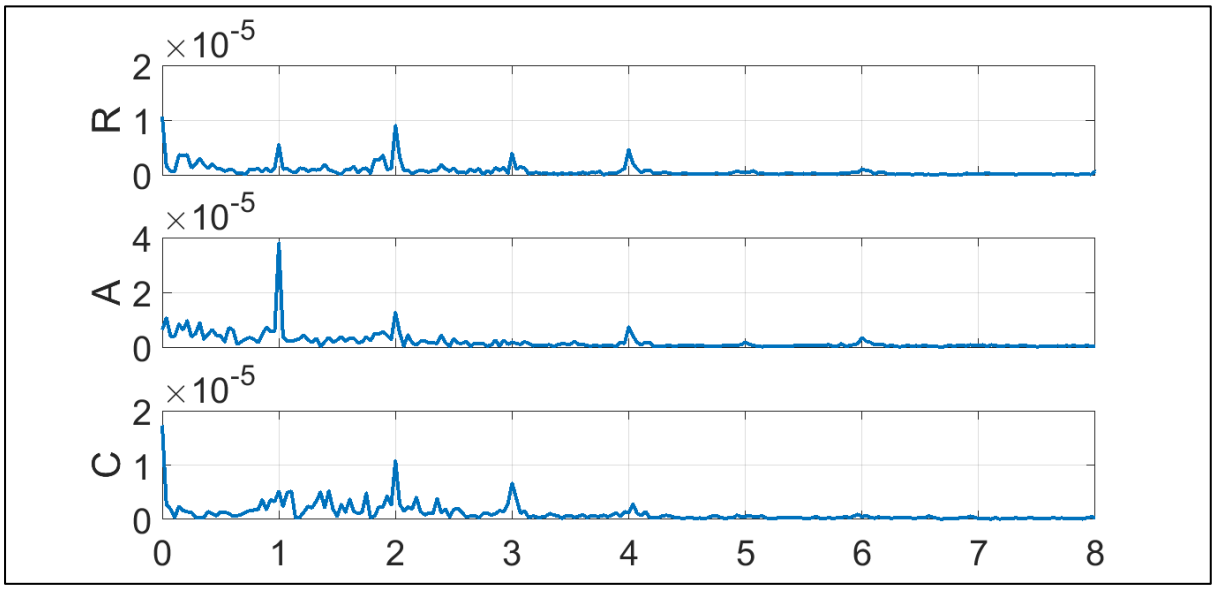

Figure 6. Spectrum of the error in the orbit components radial, along-track, and cross-track. PRN 14. On the x axis the frequencies are in unites of 1/ day.

To study what frequency has to be used in the fitting, the spectrum of the products' error was analysed. Figures 5 and 6 present the spectrum of the orbits for GPS PRN 5 and PRN 14.

A peak at twice per day frequency is visible in all the orbit components, while a peak at once per day is mainly in the along-track. Smaller peaks are also at 3 – to – 8 times per day, but they were neglected in our modelling.

Similar conclusions can be drawn by looking at the spectrum of the clocks' difference.

Hence, the error in the Real-Time products Δ_{RT} is modelled as the sum of two sinusoids with period T_E equal to the Earth rotation Period (23 hours 56 minutes) and period T_O equal to the orbital period of the constellation (11 hours 58 minutes for GPS, 14 hours 22 minutes for Galileo).

$$\Delta_{RT} = b + a_E \sin\left(\frac{2\pi}{T_E}t + \Phi_E\right) + a_O \sin\left(\frac{2\pi}{T_O}t + \Phi_O\right) \quad (6)$$

Table 2 show the average biases and amplitudes a_E and a_O for each component in the period analysed.

Table 2. RMS of the fitting parameters. a_E is the amplitude of the sinusoid with period equal to the Earth rotation period, while a_O is the amplitude of the sinusoid with period equal to the orbital period of the constellation.

	Radial	**Along-track**	**Cross-track**	**Clocks**
bias [cm]	1.48	3.99	1.92	17.31
a_E [cm]	1.30	4.17	2.22	6.64
a_O [cm]	1.04	2.11	1.62	4.36

3 Validation

The system was validated against real data recorded between GPS week 1917 and 1920. GPS observations from ten stations within the IGS global network were considered. Each daily RINEX file was split into two 6 hours data arc (0 – 6am, 12 – 6pm) and, therefore, 560 data points were analysed.

The POINT software was used to process the GNSS observations in PPP mode. This software, which was developed in the iNsight project (www.insight-gnss.org), supports multiple constellations (GPS, GLONASS, and Galileo) and multiple positioning techniques, such as Real Time Kinematic (RTK) and PPP (Jokinen et al., 2012).

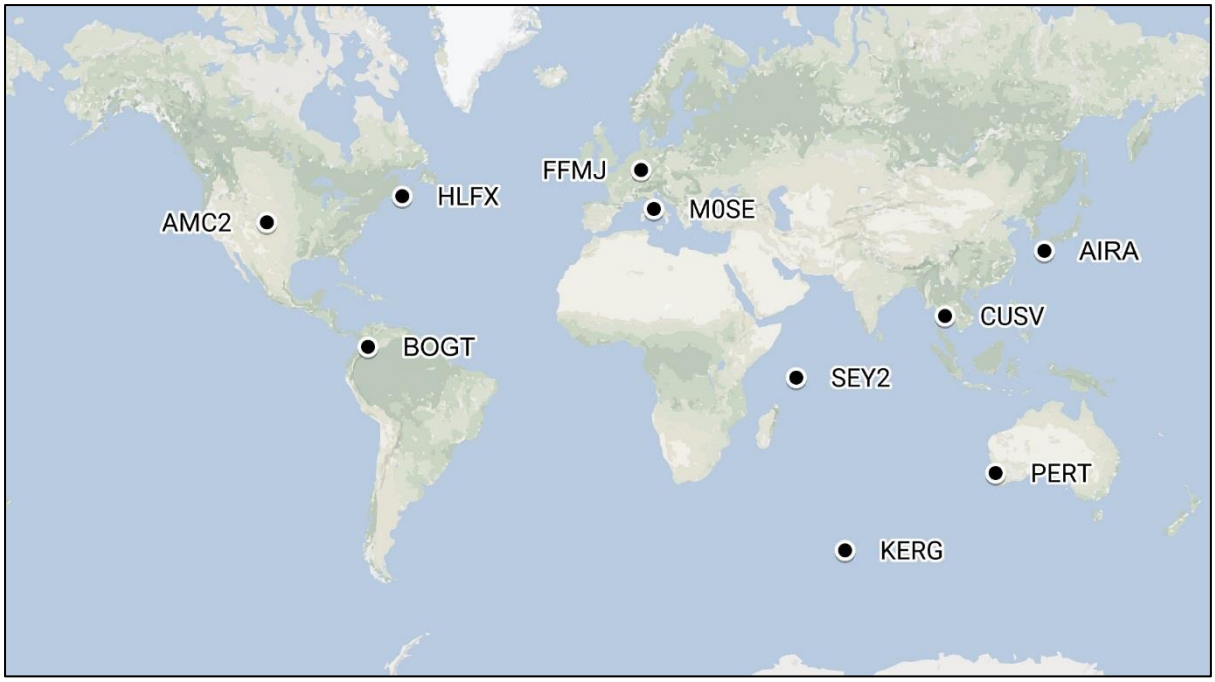

Figure 5. IGS stations considered for validation.

The metric used to analyse the positioning performance are the errors in the north, east and down component of the position at the end of the 6 hours, and the time they take to converge below one decimetre.

Table 3 and Table 4 show that the performance of the Simulink model is comparable to the real data.

Table 3. Median of the positioning errors for simulated and real data. Values in units of centimetres.

	Real data				**Simulated data**			
Station	3D	North	East	Down	3D	North	East	Down
AIRA	3.22	0.82	1.14	2.79	3.93	0.61	1.52	3.40
AMC2	4.25	1.85	2.30	2.21	3.17	0.58	1.69	2.24
BOGT	4.49	1.40	1.73	3.36	2.57	0.65	1.12	1.98
CUSV	3.90	0.69	1.54	2.79	3.62	0.36	1.28	3.01
FFMJ	2.13	0.70	0.89	1.28	4.21	0.43	1.47	3.74
HLFX	5.29	1.60	1.59	4.28	4.03	0.61	0.91	3.43
KERG	3.08	0.72	1.25	2.43	3.61	0.62	0.86	3.25
M0SE	2.79	0.68	0.69	1.81	3.16	0.57	0.91	2.76

PERT	5.07	0.75	1.89	4.33	3.49	0.48	1.60	2.76
SEY2	3.70	0.99	1.62	2.44	3.30	0.60	0.93	2.52

Table 4. Median of convergence times for simulated and real data. Values in units of minutes.

	Real data				**Simulated data**			
Station	3D	North	East	Down	3D	North	East	Down
AIRA	92	10	68	70	42	13	32	27
AMC2	66	10	27.5	45	82	16	64	64
BOGT	75	7	31	61	35	15	21	28
CUSV	59	8	30	54	53	16	27	47
FFMJ	43	7	16	25	46	13	31	26
HLFX	49	8	33	29	44	16	24	33
KERG	48	12	31	25	43	15	25	23
M0SE	69	12	34	46	62	20	44	44
PERT	116	18	28	84	40	13	32	25
SEY2	64	8	30	40	41	11	17	38

4 Multi – Constellation PPP results

The PPP solutions based on the ionosphere free (IF) combination between GPS L1 and L5 signals only, Galileo E1 and E5a or E1 and E5 only, or GPS and Galileo signals combined are analysed. The simulated observations from the same ten stations as in validation stage were processed with the POINT software in static mode with float ambiguity. Open sky condition was assumed. For, each station, the simulator was run 55 times.

For static processing, the metrics used to define the positioning performance are the errors in the north, east and down components of the position at the end of the processing and the time these errors take to converge below 10 cm level.

In Figures 7 and 8 is a comparison between the RMS of the errors and convergence times for each position's component and for the different signals combinations for station PERT and HLFX.

Each combination is able to provide sub-decimetre level accuracy after few tens of minutes. The convergence time in the vertical direction is usually the longest, it ranges from 24 minutes for the multi-constellation solution to 75 minutes for GPS L1 – L5 IF, both in HLFX.

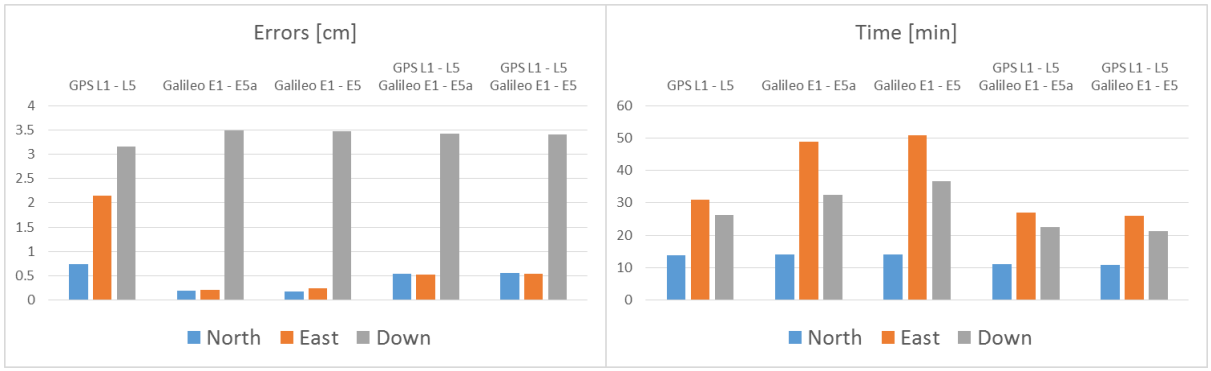

Figure 7. Errors and convergence times for different signals combinations: in the first block is GPS L1 – L5 IF, the second refers to Galileo E1 – E5a IF, in the third is Galileo E1 – E5 IF, in the fourth is GPS L1 – L5 IF plus Galileo E1 – E5a IF, and the last block is GPS L1 – L5 IF plus Galileo E1 – E5 IF. Station PERT.

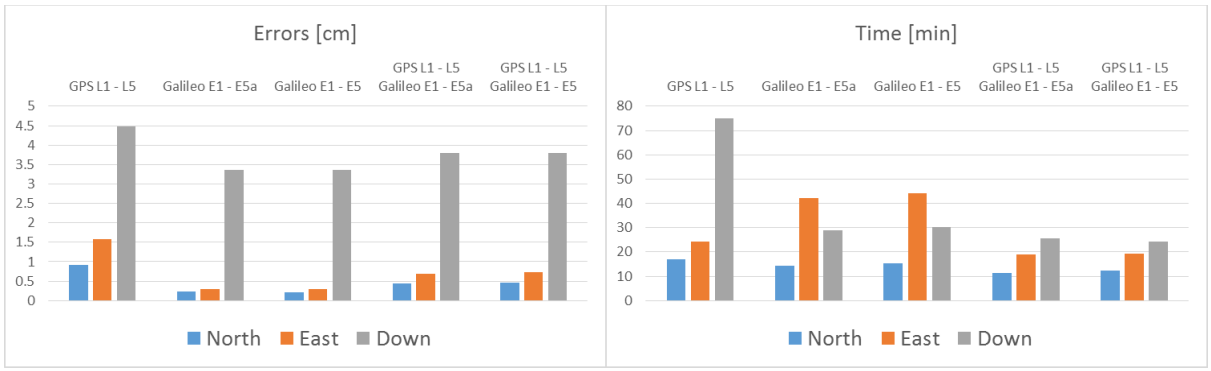

Figure 8. Errors and convergence times for different signals combinations: in the first block is GPS L1 – L5 IF, the second refers to Galileo E1 – E5a IF, in the third is Galileo E1 – E5 IF, in the fourth is GPS L1 – L5 IF plus Galileo E1 – E5a IF, and the last block is GPS L1 – L5 IF plus Galileo E1 – E5 IF. Station HLFX.

In eight stations out of ten considered, positioning with Galileo E1 – E5a IF performs better than GPS L1 – L5 IF, both in terms of accuracy and convergence time. Up to 33% and 29% of improvement, respectively, in the down accuracy level and convergence time can be observed when processing the Galileo E1 – E5a IF compared to GPS L1 – L5 IF. PERT is the only one station where GPS outperforms Galileo in both vertical accuracy and convergence time, while in FFMJ Galileo has worse vertical accuracy but faster convergence time than GPS. The reason why Galileo, in general, performs so much better than GPS has to be addressed to its lower noise that was assumed in the code pseudoranges (Richardson et al., 2016).

Given the open sky condition, there were not much improvements in terms of Dilution of Precision (DOP) when the two constellations where used together respect to the single

constellation case (see Figure 9), therefore the accuracy achieved is mostly sensitive to the quality of the pseudoranges. For this reason, it is mainly the convergence time taking benefit from using GPS and Galileo together. On average over all the considered stations, the convergence time was 47% faster than GPS only solution and 26% faster than the Galileo only solution.

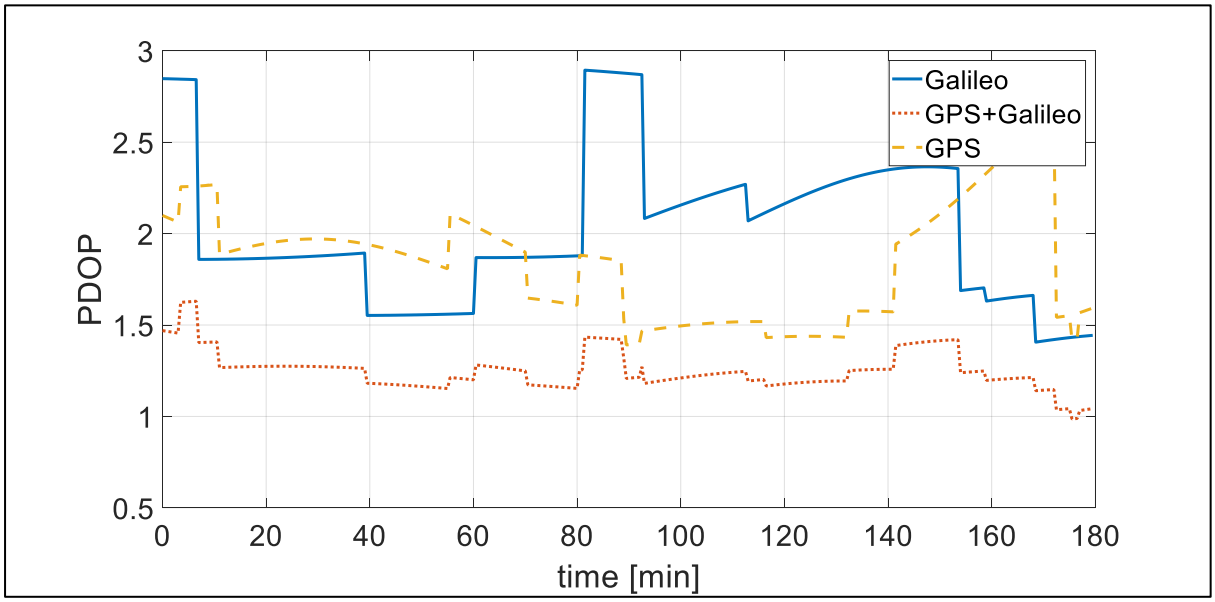

Figure 9. Galileo only, GPS only and GPS plus Galileo Position Dilution of Precision (PDOP). Station HLFX.

By employing the Galileo E1 – E5 IF no benefit to the positioning solution were registered in comparison with the E1 – E5a solution. From simulated analysis, the two combinations have nearly the same performance. The reason can be found in IF combination, which is well known to degrade the quality of the measurements.

5 Concept of smoothed ionosphere correction for fast reconvergence

In order to shorten the convergence time, ambiguity fixing method have been developed in recent years (Collins et al., 2010, Laurichesse et al., 2009, Ge et al., 2008). These methods are all based on the ionosphere free combination.

However, the results presented in the previous section demonstrate that the convergence time in PPP would be shorter if we could use less noisy pseudoranges. Therefore, the use of the IF combination, which can amplify the noise in the measurements up to 3 times, limits the potential performance of PPP. Obviously, this is well accepted as it is the best option available to mitigate the ionospheric delay in the observables. As an alternative, PPP algorithms in which

the ionospheric delays were provided by Global Ionospheric Map (GIM) (Teunissen et al., 2010, Wubbena et al., 2005) or estimated in the state vector (Geng et al., 2010, Li et al., 2013, Zhang et al., 2013) were proposed. The performance of these approaches not only depends on the quality of the GIM or the spatial and temporal constraints used for the ionosphere estimation, but also on a careful handling of the differential code biases (DCBs), as pointed in Zhang et al. (2013).

Here a new method to mitigate the ionosphere and aimed to reduce the reconvergence time, after initial convergence has been achieved, is proposed. Reconvergence is important in situations such as mobile platforms operating in urban environments.

The IF combination P_3 between two pseudoranges P_1 and P_2 on frequencies f_1 and f_2 can be computed according to Equation 7.

$$P_3 = \frac{f_1^2}{f_1^2 - f_2^2} P_1 - \frac{f_2^2}{f_1^2 - f_2^2} P_2 \tag{7}$$

This formulation is equivalent to correcting the pseudorange P_1 with the ionospheric delay computed from the geometry free combination.

$$P_3 = P_1 - I_1^P \tag{8}$$

$$I_1^P = \frac{P_1 - P_2}{1 - \frac{f_1^2}{f_2^2}} \tag{9}$$

In this new method, the ionospheric correction is smoothed through a Hatch filter (Hatch, 1982) before being applied to the pseudorange. The opposite sign of the ionospheric delay in the code pseudorange and carrier phase needs to be considered to avoid the divergence problem (McGraw et al., 2013). In Equation (10), $\tilde{I}_{1,k}$ is the smoothed ionosphere at epoch k, $I_{1,k}^P$ is the ionosphere computed from the pseudoranges at epoch k, according to Equation (9), $I_{1,k}^L$ is the ionosphere computed from the carrier phase measurements, as in Equation (11), finally n is the size of the smoothing window.

$$\tilde{I}_{1,k} = \frac{1}{n} I_{1,k}^P + \left(1 - \frac{1}{n}\right) \cdot (\tilde{I}_{1,k-1} + \left(I_{1,k}^L - I_{1,k-1}^L\right) \tag{10}$$

$$I_{1,k}^{L} = -\frac{L_1 - L_2}{1 - \frac{f_1^2}{f_2^2}} \tag{11}$$

In this way, we can choose a smoothing window as large as the whole observation period without being affected by the divergence, as demonstrated in Figure 10.

Once the Hatch filter has converged, ideally we have IF pseudoranges with up to three times less noise than the traditional IF combination.

Therefore, in case the receiver loses track of all the satellites and the PPP filter needs to be restarted, we can take advantage of this new low noise IF pseudorange to obtain a quicker reconvergence, rather than having tens of minutes with meter or decimetre level accuracy. Indeed, provided that the signal gap is not very large, the Hatch filter applied to the ionosphere delay doesn't need to be reinitialized from the raw values if a cycle slip occurs. The old information about how the ionosphere changes with the time can be used to propagate even in case of a cycle slip, since the change of rate of the ionosphere doesn't vary that much from epoch to epoch.

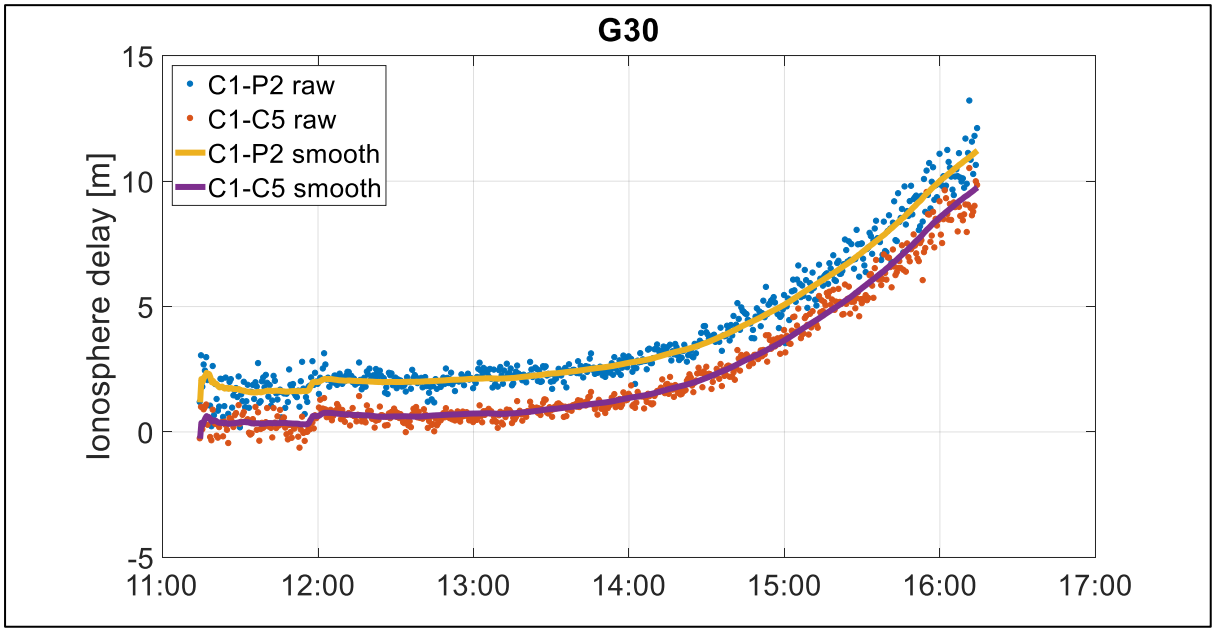

Figure 10. Ionosphere delay computed from C1 – P2 combination (raw blue dots, smoothed yellow line) and C1 – C5 combination (raw orange dots, smoothed purple line). GPS PRN 30 observed from BOGT on the 6th September 2016. On that day a minor solar storm made the ionosphere pretty active. The offset between the two plots is due to the DCBs.

6 Preliminary results

To test the benefit of this new method on the reconvergence time, 3 hours of simulated Galileo data were processed with the POINT software in kinematic mode. After 90 minutes, the PPP filter was force to restart to simulate reconvergence. The performance of the traditional E1 – E5 IF were compared with those of E1 and E5 corrected with smoothed ionosphere delay coming from the Hatch filter. Figures 11, 12 and 13 show the precision (3σ) of the north, east and down component after filter restart. In all three components, the new approach show faster reconvergence respect to the traditional PPP based on the IF combination.

In particular, the horizontal components for the E5 plus Hatch case converge below 10 cm accuracy immediately. While the vertical component takes only 240 seconds to reach an accuracy of 25 cm for 99% of the time, against 900 seconds for the E1 – E5 IF combination. Big improvements are also visible if we consider the noisier E1 signal. The horizontal components reconverge to below 10 cm in less than 200 seconds and the vertical component takes 700 seconds to go below 25 cm.

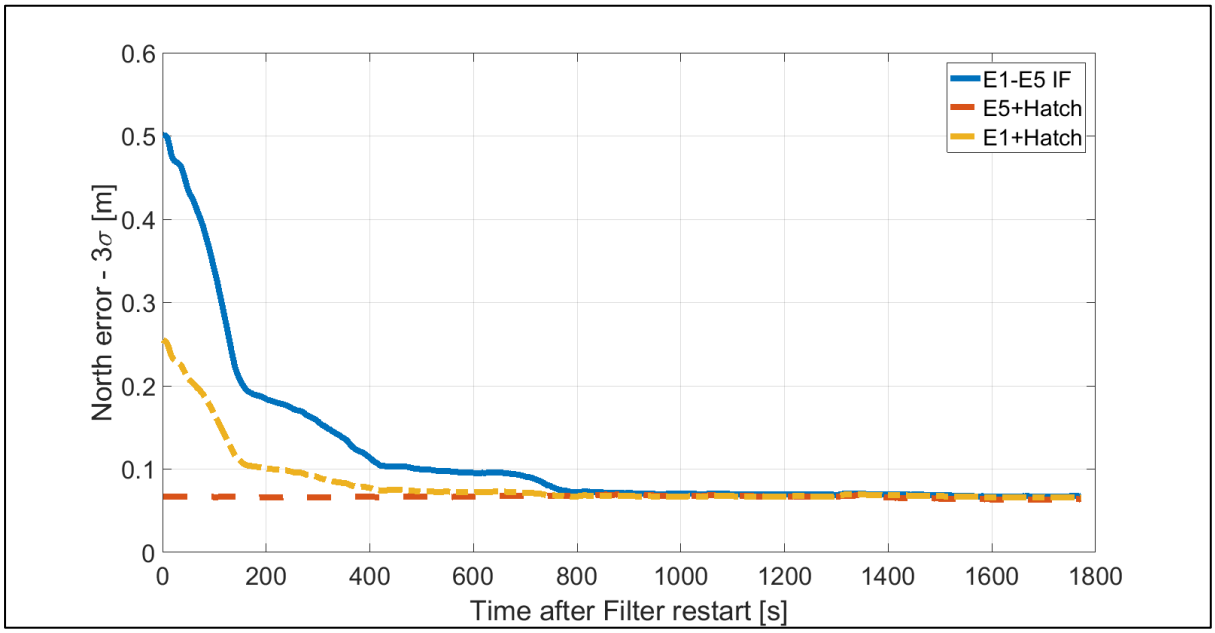

Figure 11. Comparison between the accuracy level provided by the traditional E1 – E5 IF, the E1 plus Hatch filter configuration and the E5 plus Hatch configuration after the PPP filter was forced to restart. North component. The standard deviation at epoch e is computed between e and e plus 30 minutes.

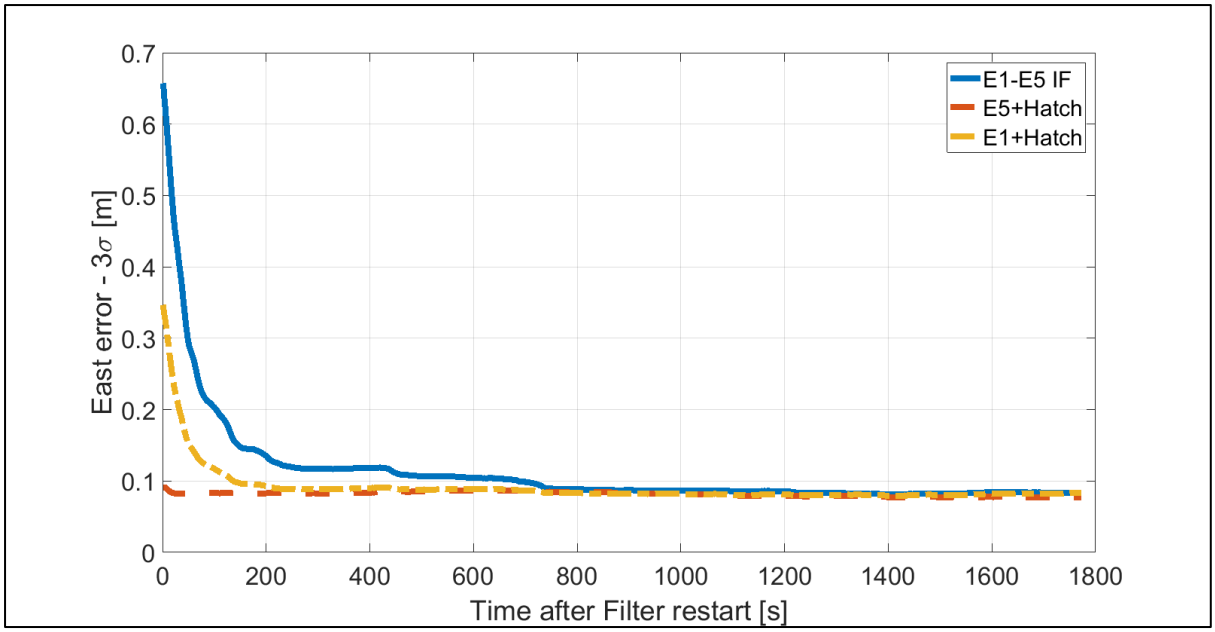

Figure 12. Comparison between the accuracy level provided by the traditional E1 – E5 IF, the E1 plus Hatch filter configuration and the E5 plus Hatch configuration after the PPP filter was forced to restart. East component. The standard deviation at epoch e is computed between e and e plus 30 minutes.

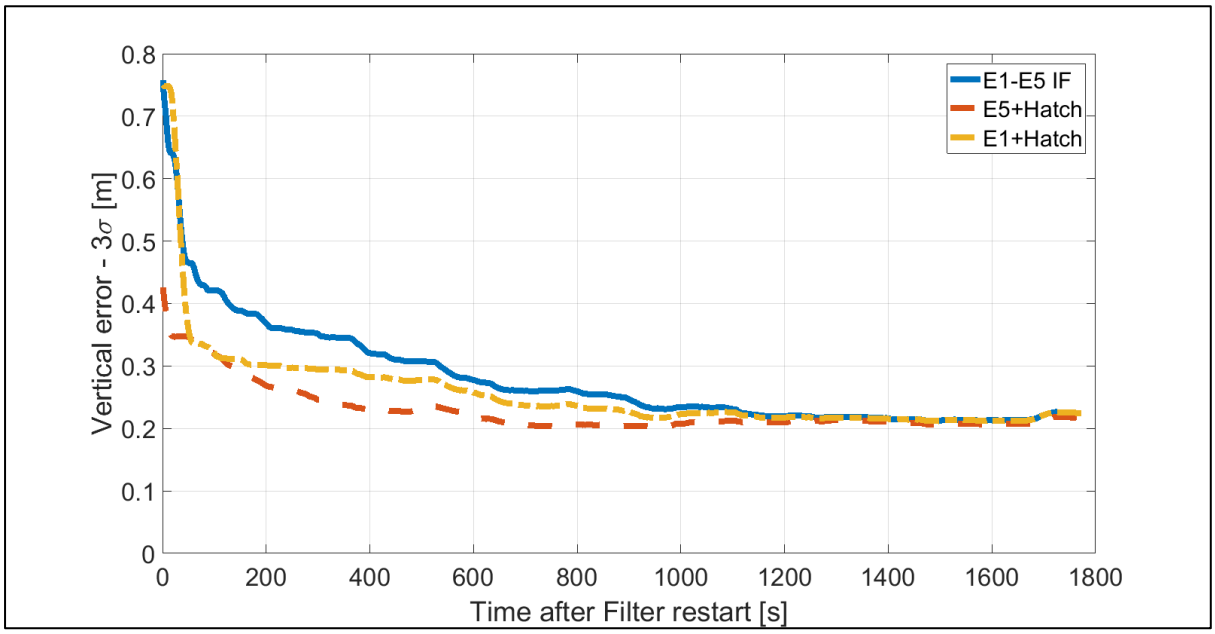

Figure 13. Comparison between the accuracy level provided by the traditional E1 – E5 IF, the E1 plus Hatch filter configuration and the E5 plus Hatch configuration after the PPP filter was forced to restart. Down component. The standard deviation at epoch e is computed between e and e plus 30 minutes.

7 Conclusions

In order to study the potential performance of Galileo signals in PPP, a simulator for GNSS measurements and precise products was developed.

The analysis made on the GPS Real-Time products showed that the two major component of their error have periods equal to the orbital period of the GPS constellation and the Earth rotation period.

Preliminary results in open sky condition, demonstrated that on average Galileo signals perform better than GPS signals, both in terms of accuracy and convergence time. This was addressed to the better quality of Galileo pseudoranges. Also, using the two system combined improves mostly the convergence time. Finally, it was noted that the use of the IF combination with E1 limits the potentials of Galileo E5 signal.

Starting from these results, a new PPP approach based on pseudoranges corrected by a smoothed ionospheric delay was proposed. This configuration seems to provide faster reconvergence compared to the traditional PPP with the IF combination.

Acknowledgements

The authors would like to thank Dr. Gary McGraw and Andrew Johnson from the Rockwell Collins for their help, supervision and comments during the preparation of this paper.

References

AFIFI, A. & EL-RABBANY, A. 2015. Performance Analysis of Several GPS/Galileo Precise Point Positioning Models. *Sensors (Basel),* 15**,** 14701-26.

COLLINS, P., BISNATH, S., LAHAYE, F. & HÉROUX, P. 2010. Undifferenced GPS Ambiguity Resolution Using the Decoupled Clock Model and Ambiguity Datum Fixing. *Navigation,* 57**,** 123-135.

ESA. 2015. *Salvage in Space: Recovering Galileo 5 and 6* [Online]. Available: http://esamultimedia.esa.int/docs/galileo/Galileo_Sav_flyer_j15_low-res.pdf [Accessed].

GE, M., GENDT, G., ROTHACHER, M., SHI, C. & LIU, J. 2008. Resolution of GPS carrier-phase ambiguities in Precise Point Positioning (PPP) with daily observations. *Journal of Geodesy,* 82**,** 389-399.

GENG, J., MENG, X., DODSON, A. H., GE, M. & TEFERLE, F. N. 2010. Rapid re-convergences to ambiguity-fixed solutions in precise point positioning. *Journal of Geodesy,* 84**,** 705-714.

GSA. 2014. *Notice Advisory for Galileo Users (NAGU) 2014014* [Online]. Available: https://www.gsc-europa.eu/sites/default/files/NOTICE_ADVISORY_TO_GALILEO_USERS_NAGU_2014014.txt [Accessed].

GSA. 2016a. *Notice Advisory for Galileo Users (NAGU) 2016029* [Online]. Available: https://www.gsc-europa.eu/sites/default/files/NOTICE_ADVISORY_TO_GALILEO_USERS_NAGU_2016029.txt [Accessed].

GSA. 2016b. *Notice Advisory for Galileo Users (NAGU) 2016030* [Online]. Available: https://www.gsc-europa.eu/sites/default/files/NOTICE_ADVISORY_TO_GALILEO_USERS_NAGU_2016030.txt [Accessed].

HADAS, T. & BOSY, J. 2015. IGS RTS precise orbits and clocks verification and quality degradation over time. *GPS Solutions,* 19**,** 93-105.

HATCH, R. The synergism of GPS code and carrier measurements. International Geodetic Symposium on Satellite Doppler Positioning, 1982 Las Cruces, NM, USA. 1213-1231.

JOKINEN, A., FENG, S., OCHIENG, W., HIDE, C., MOORE, T. & HILL, C. 2012. Fixed ambiguity Precise Point Positioning (PPP) with FDE RAIM. *ION PLANS.* Myrtle Beach, SC: IEEE.

JUAN, J. M., HERNANDEZ-PAJARES, M., SANZ, J., RAMOS-BOSCH, P., ARAGON-ANGEL, A., ORUS, R., OCHIENG, W., FENG, S., JOFRE, M., COUTINHO, P., SAMSON, J. & TOSSAINT, M. 2012. Enhanced Precise Point Positioning for GNSS Users. *IEEE Transactions on Geoscience and Remote Sensing,* 50**,** 4213-4222.

LAURICHESSE, D., MERCIER, F., BERTHIAS, J.-P., BROCA, P. & CERRI, L. 2009. Integer Ambiguity Resolution on Undifferenced GPS Phase Measurements and Its Application to PPP and Satellite Precise Orbit Determination. *Navigation,* 56**,** 135-149.

LI, X., GE, M., ZHANG, H. & WICKERT, J. 2013. A method for improving uncalibrated phase delay estimation and ambiguity-fixing in real-time precise point positioning. *Journal of Geodesy,* 87**,** 405-416.

MCGRAW, G., SCHNAUFER, B. A., HWANG, P. Y. & ARMATYS, M. J. Assessment of Alternative Positioning Solution Architectures for Dual Frequency Multi-Constellation GNSS/SBAS. International Technical Meeting of The Satellite Division of the Institute of Navigation, 2013 Nashville, TN, USA. 223-232.

MIGUEZ, J., GISBERT, J. V. P., PEREZ, R. O., GARCIA-MOLINA, J. A., SERENA, X., GONZALES, F., GRANADOS, G. S. & CRISCI, M. Multi-GNSS PPP Performance Assessment with Different Ranging Accuracies in Challenging Scenarios. International Technical Meeting of The Satellite Division of the Institute of Navigation, 2016 Portland, OR, USA. 2069-2081.

MONTENBRUCK, O., RIZOS, C., WEBER, R., WEBER, G., NEILAN, R. E. & HUGENTOBLER, U. 2013. Getting a Grip on Multi-GNSS: the International GNSS Service MGEX Campaign. *GPS world,* 24**,** 44-49.

MONTENBRUCK, O., STEIGENBERGER, P., KHACHHIKYAN, R., WEBER, G., LANGLEY, R., MERVART, L. & HUGENTOBLER, U. 2014. IGS-MGEX: Preparing the Ground for Multi-Constellation GNSS Science. *Inside GNSS,* 9**,** 42-49.

O'KEEFE, K., PETOVELLO, M., LACHAPELLE, G. & CANNON, M. E. 2006. Assessing Probability of Correct Ambiguity Resolution in the Presence of Time-Correlated Errors. *Navigation,* 53**,** 269-282.

RICHARDSON, T., HILL, C. & MOORE, T. Analysis of Multi-Constellation GNSS Signal Quality. International Technical Meeting of The Institute of Navigation, 2016 Monterey, CA, USA. 631-638.

RIZOS, C., MONTENBRUCK, O., WEBER, R., WEBER, G., NEILAN, R. E. & HUGENTOBLER, U. The IGS MGEX Experiment as a Milestone for a Comprehensive Multi-GNSS Service. ION Pacific PNT Meeting, 2013 Honolulu, Hawaii. 289-295.

SHEN, X. & GAO, Y. Analyzing the Impacts of Galileo and Modernized GPS on Precise Point Positioning. National Meeting of the Institute of Navigation, 2006 Monterey, CA, USA. 837-846.

SIMSKY, A., MERTENS, D., SLEEWAEGEN, J.-M., HOLLREISER, M. & CRISCI, M. 2008. Experimental Results for the Multipath Performance of Galileo Signals Transmitted by GIOVE-A Satellite. *International Journal of Navigation and Observation,* 2008**,** 1-13.

TEUNISSEN, P. J. G. & MONTENBRUCK, O. 2017. *Springer Handbook of Global Navigation Satellite Systems*, Springer International Publishing.

TEUNISSEN, P. J. G., ODIJK, D. & ZHANG, B. 2010. PPP-RTK: Results of CORS Network-Based PPP with Integer Ambiguity Resolution. *Journal of Aeronautics, Astronautics and Aviation,* 42**,** 223 - 230.

WUBBENA, G., SCHMITZ, M. & BAGGE, A. PPP-RTK: Precise Point Positioning Using State-Space Representation in RTK Networks. International Technical Meeting of the Satellite Division of The Institute of Navigation (ION GNSS), 2005 Long Beach, CA. 2584 - 2594.

ZHANG, H., GAO, Z., GE, M., NIU, X., HUANG, L., TU, R. & LI, X. 2013. On the convergence of ionospheric constrained precise point positioning (IC-PPP) based on undifferential uncombined raw GNSS observations. *Sensors (Basel),* 13**,** 15708-25.

ZUMBERGE, J. F., HEFLIN, M. B., JEFFERSON, D. C., WATKINS, M. M. & WEBB, F. H. 1997. Precise point positioning for the efficient and robust analysis of GPS data from large networks. *Journal of Geophysical Research: Solid Earth,* 102**,** 5005-5017.